scientific reports

Check for updates

OPEN

Genetic editing of primary human dorsal root ganglion neurons using CRISPR-Cas9

Seph M. Palomino[1,7], Katherin A. Gabriel[2,7], Juliet M. Mwirigi[2], Anna Cervantes[3], Peter Horton[3], Geoffrey Funk[3], Aubin Moutal[4], Laurent F. Martin[5], Rajesh Khanna[6], Theodore J. Price[2]✉ & Amol Patwardhan[1]✉

CRISPR-Cas9 is now the leading method for genome editing and is advancing for the treatment of human disease. CRIPSR has promise in treating neurological diseases, but traditional viral-vector-delivery approaches have neurotoxicity limiting their use. Here we describe a simple method for non-viral transfection of primary human DRG (hDRG) neurons for CRISPR-Cas9 editing. We edited *TRPV1*, *NTSR2*, and *CACNA1E* using a lipofection method with CRISPR-Cas9 plasmids containing reporter tags (GFP or mCherry). Transfection was successfully demonstrated by the expression of the reporters two days post-administration. CRISPR-Cas9 editing was confirmed at the genome level with a T7-endonuclease-I assay; protein level with immunocytochemistry and Western blot; and functional level through capsaicin-induced Ca^{2+} accumulation in a high-throughput compatible fluorescent imaging plate reader (FLIPR) system. This work establishes a reliable, target specific, non-viral CRISPR-Cas9-mediated genetic editing in primary human neurons with potential for future clinical application for sensory diseases.

Genome editing techniques have revolutionized the biomedical field, expanding our knowledge of human diseases and providing therapeutic applications in humans. Clustered regularly interspaced short palindromic repeats (CRISPR) - CRISPR associated protein 9 (Cas9) is a genome editing technique that uses a guide RNA (gRNA) to efficiently induce double stranded breaks in DNA, driving activation of DNA repair systems that can introduce site specific genomic modifications[1,2]. CRISPR-Cas9 systems have been widely utilized in understanding various disease related pathways and have accelerated application of genetically engineered cells and organisms. Previously, screening in both cell lines and primary cultures mostly involved small interfering RNA (siRNA), or RNAi, to investigate loss-of-function or drug activity of specific target proteins; However, the approach involves extensive troubleshooting to predict its partial knockdown effect, off-target effects, and is limited to protein-coding genes[3,4]. Cas9-mediated CRISPR tools are now widely used in screening due to their efficiency and ability to target the entire genome[5,6]. CRISPR-Cas9 has now entered therapeutic era with successful treatment of sickle cell disease and β-thalassemia[7–10]. Despite these important advances, two of the biggest challenges encountered in genome editing are low transfection efficiency and toxicities arising from delivery strategies. These issues are particularly relevant for the nervous system because neurons are challenging to transfect without viral vectors and dorsal root ganglion toxicities from viral vectors have presented challenges in clinical trials and in preclinical development in non-human primate species[11–15].

There are several transduction/transfection methods available for CRISPR-Cas9 and they are divided into two broad categories: viral and non-viral[16]. Viral transduction uses a viral vector to carry a specific DNA sequence into the host cells. For stable transductions retroviruses and lentiviruses are used, while baculoviruses and adeno-associated viruses (AAVs) are used for transient transductions[16]. LVs have been a powerful tool used for gene editing in mammals and the use of the non-integrating LVs has reduced the chances of insertion related mutations[17]. Baculoviruses, commonly used in insects and insect cell lines, have been further developed for use of CRISPR editing in mammalian cell lines, but have not been tested in human primary neurons[18–22]. The AAVs

[1]Department of Anesthesiology and Pain Management, University of Texas Southwestern Medical Center, 6202 Harry Hines Blvd., 9th Floor, Dallas 75235, TX, USA. [2]Department of Neuroscience and Center for Advanced Pain Studies, University of Texas at Dallas, 800 W Campbell Rd, Richardson, TX 75080, USA. [3]Southwest Transplant Alliance, Manderville Ln, Dallas, TX 8190, 75231, USA. [4]Department of Pharmacology and Physiology, Saint Louis University, 1402 S. Grand Blvd, St. Louis, Mo 63104, USA. [5]Department of Pharmacology, University of Arizona, 1501 N Campbell Ave, Tucson, AZ 85721, USA. [6]Department of Pharmacology and Therapeutics, University of Florida, 1200 Newell Drive, Gainesville, FL ARB R5-234, 32610-0267, USA. [7]Seph M. Palomino and Katherin A. Gabriel contributed equally to this work. ✉email: theodore.price@utdallas.edu; amol.patwardhan@utsouthwestern.edu

are widely recognized as highly effective at achieving transduction on notoriously difficult to transfect primary cells, such as neurons and have been shown to be applicable in vivo[23,24]. Viral vectors have been great tools for research with the potential to be used clinically for gene therapy.

The dorsal root ganglion (DRG) is an important peripheral nervous tissue attached to the spinal cord containing the cell bodies of primary afferent sensory neurons relaying inputs such as temperature, touch, pain, and itch as well as motor outputs, and is a common source of primary neuronal cultures[25]. Transfections using AAVs have led to major toxicities in DRG clinically, a relevant concern of this approach[11–15]. For non-viral transfection methods, the options are mechanical, physical, or chemical transfections. Electroporation is the best-known physical method used to transfect cells and has been recently used to create the CRISPR-Cas9–edited $CD34^{+}$hematopoietic stem cells used in a sickle cell disease clinical trial[10]. Sonoporation, laser, or magnet -assisted transfection are also common methods but can irreversibly damage the cell membrane and have low transfection efficiency[26]. Likewise, Virus-like particles (VLPs) have also been used both in-vivo and in-vitro as delivery systems; however, the purification process can yield low functional VLPs making them not as efficient[27,28]. Though, viral like particles for CRISPR-Cas9 delivery in neuronal cells in-vivo have proven to be successful[29]. Similarly, nucleofection has been shown to successfully deliver CRISPR-Cas9 editing technology in primary neuronal culture from rodents to fluorescently label proteins[30]. Chemical transfections now mostly rely on lipid-based methods where positively charged lipid particles fuse with the phospholipid bilayer and enable the genetic material to easily enter the cell[16]. Lipid-based nanoparticle approaches are used medically for vaccine delivery, gene therapy and are used in clinical trials for a variety of diseases[31,32].

We sought to develop a viral-vector-independent method for CRISPR-Cas9 editing in human DRG neurons recovered from organ donors. Our work was motivated by the need for a genome editing technique for discovery work utilizing human primary neurons, and for pre-clinical application in pain studies. To these ends, we describe a non-viral, lipofectamine-based transfection method for CRISPR-Cas9 genome editing in primary human DRG neurons. Successful transfection was verified by the expression of reporter protein and by mismatch insertion and deletion (indel) assay. We verified genetic editing at the protein level via immunocytochemistry and Western blotting demonstrating up to a 70% decrease in protein expression over a 5-day period after editing. Lastly, we demonstrate a functional loss of TRPV1 expression using a capsaicin-evoked Ca^{+2} imaging FLIPR assay. Our findings reveal a new method that can be used for assessment of gene and associated protein function directly in human sensory neurons, ideal for screening drug action on human sensory neurons that can aid discovery in diseases like intractable pain.

Results

CRISPR-Cas9 transfection protocol and viability in human DRG cultures

Human DRG (hDRG) cultures were prepared through recovery of lumbar and thoracic DRGs from 13 organ donors (Supplementary Table 1). The hDRGs were collected and immediately placed in cold (~4 °C) bubbled aCSF then transported to the laboratory for processing. Human DRG neuronal cultures were prepared as described previously (Supplementary Fig. 1)[33]. We selected the transient receptor potential vanilloid 1 channel (*TRPV1*) as our first genetic target of interest due to its high expression in the hDRGs[34]and for its specific and thoroughly validated agonist, capsaicin[35–37]. The CRISPR construct, designed by GeneCopoeia, contains a U6 promoter followed by a single guide RNA for the target of interest and the reporter tag gene for mCherry; The Cas9 nuclease gene is driven by a CMV promoter. All CRISPR constructs were obtained in a BSL-1 *E. coli* bacterial vector, the DNA plasmid was amplified through growth of the vector through ampicillin selective growth media and extracted using a maxi prep Qiagen kit.

Our group's experimental timeline is outlined in Fig. 1a. We chose a cationic lipid-based transfection method, using lipofectamine3000, to insert the plasmids into the cells present in the hDRG cultures. The concentration of the plasmid DNA to transfect the cells ranged from 0.5 to 5 µg depending on the size of the culture dishes and relative cell number. The amount of lipofectamine3000 was adjusted according to media volume and surface area of the culture dishes; the formulation of the plasmid-transfection reagent was adjusted according to the manufacturer's recommendations and diluted in serum free BrainPhys culture media (Fig. 1b) (Table 1)**.** The extracted CRISPR-Cas9 plasmid was mixed with the P3000 reagent (2uL/ug DNA) and diluted in serum free BrainPhys culture media. The media containing lipofecitimine3000 and media containing the DNA-p3000 complex were mixed at a 1:1 ratio and incubated for 15 min at room temperature. At least half of the media was removed from the wells before the DNA-lipid complex was added and incubated for 5 min at room temperature. The wells were then filled with fresh media and left for 24 h in the incubator before a full media change. We compared the overall neuronal yield from each hDRG cultured across different age groups and determined that older donors produce a lower neuronal yield (Fig. 1c). This information led us to set an age limit of 50 years old to maximize yield and survivability of neurons in culture.

Validation of CRISPR-Cas9 transfection with reporter Tag and T7 endonuclease assay

Next, to determine if the health of the culture was affected by the number of days the cells were exposed to the plasmid/lipid complex, we performed a cell viability MTS assay. This assay enabled us to calculate the change in viability of the cells before and after CRISPR-Cas9 and/or cationic lipid treatment with either 24- or 48-hour exposure time (Fig. 2a). To validate the plasmid transfection of hDRG neurons, we looked for expression of the mCherry reporter tag in the DRG cultures exposed to the DNA-lipid complex and compared them to cultures that received lipofectamine without plasmid DNA (negative control). A common characteristic of primary neuronal cultures is the presence of autofluorescence due to lipofuscin, a lipid containing pigment that accumulates in the cytoplasm due to aging[38]. The lipofuscin can be seen in the bright field images (left) as the darker pigmented areas in the neurons, and the corresponding autofluorescence in the fluorescent images (right) (Fig. 2b). Aside from the autofluorescence from the lipofuscin, compared to the negative CRISPR control,

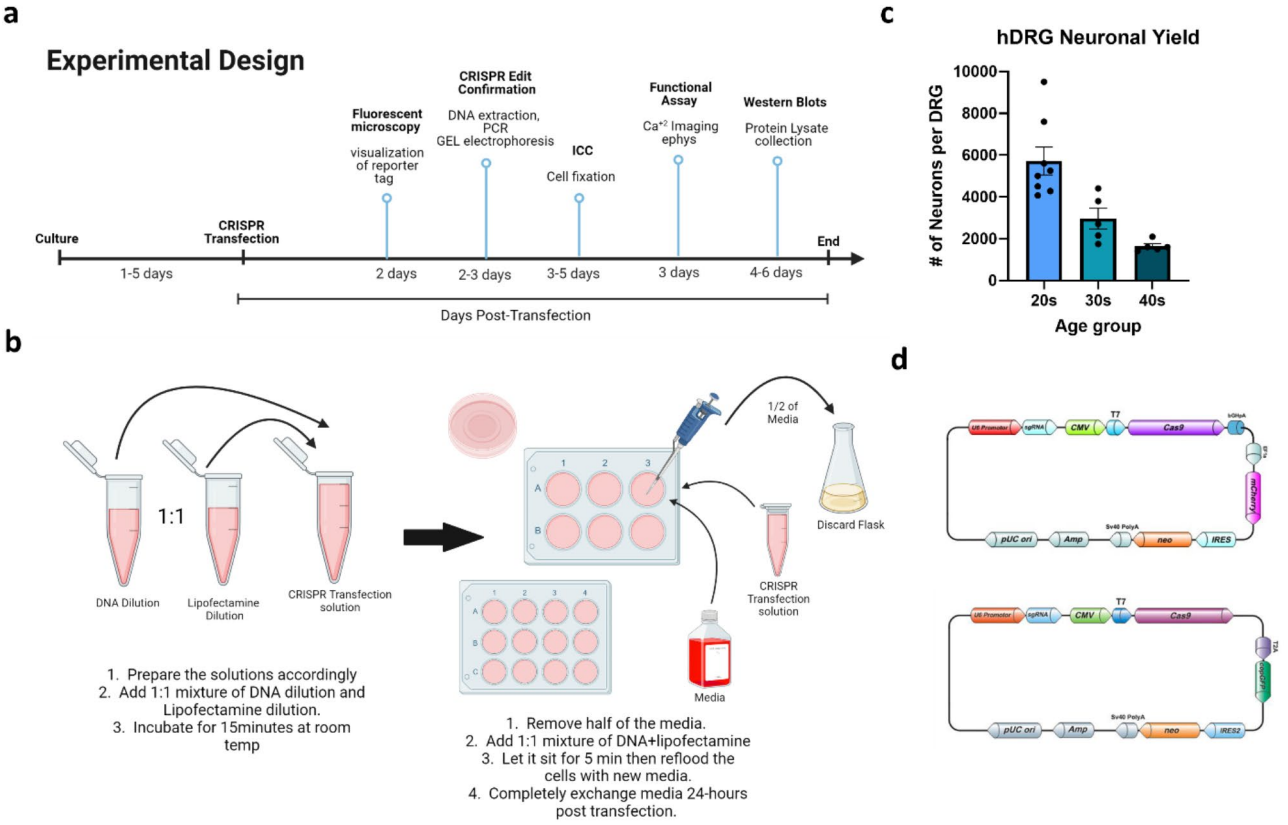

Fig. 1. CRISPR-Cas9 Transfection experimental design and Protocol. **a**. General experimental timeline of CRISPR-Cas9 transfection in hDRG culture and each consequent experimental verification steps **b**. Visual representation of transfection reagent and CRISPR plasmid formulation; a 1:1 mixture of DNA dilution and lipofectamine dilution incubated for 15 min before added to the hDRG cultured cells and incubated for 24 h.**c**. Measurement of neuronal yield per one hDRG dissociated across 3 different age groups. Each dot represents the neuronal yield for a single donor. **d.** Plasmid maps for CRISPR-Cas9 gene editing, one containing an mCherry reported tag and another containing a GFP reporter tag. Plasmid map images were obtained from GeneCopoeia website.

Component	96-Well Plate	12-Well Plate	6-Well Plate	
BrainPhys Media	4.85uL	58.5uL	121.5uL	Dilute lipofectamine in media and mix well.
Lipofectamine 3000	0.15uL	1.5uL	3.75uL	
BrainPhys Media	Adj to 5uL	Adj to 60uL	Adj to 125uL	Dilute DNA in media and add p3000 Accordingly.
DNA*	0.5-1ug	1.5-3ug	3-5ug	
P3000 Reagent	2uL/ug of DNA	2uL/ug of DNA	2uL/ug of DNA	
Diluted DNA	5uL	60uL	125uL	Add 1:1 mixture and incubate for 15 min
Diluted Lipofectamine	5uL	60uL	125uL	

Table 1. Lipofectamine 3000 reagent protocol. The hDRG cells were transfected according to these optimized specifications.

the *TRPV1* gRNA transfected cells showed a robust expression of the mCherry tag showing greater than 60% transfection efficiency (Fig. 2b, c). Since the primary cultures are a mixed culture, we quantified the expression of the reporter tag to determine the transfection efficiency in neurons alone (77%), and in the entire culture including neurons (culture)(63%) (Fig. 2c). Expression of the tag was observed two days post-transfection. These findings demonstrate that a lipid transfection method was successful in delivering DNA plasmid into cells of a primary hDRG culture.

To verify genetic editing, we chose to use a T7 endonuclease I enzyme which recognizes and cleaves mismatched DNA. We extracted DNA from the culture two days post-transfection after reporter tag expression was confirmed. Post DNA extraction, we generated PCR products using primers flanking the targeted gene sequences, then used heat denaturation followed by a room temperature re-annealing step allowing them to generate mismatched double stranded DNA fragments which can be visualized in an agarose gel (Fig. 2d). The

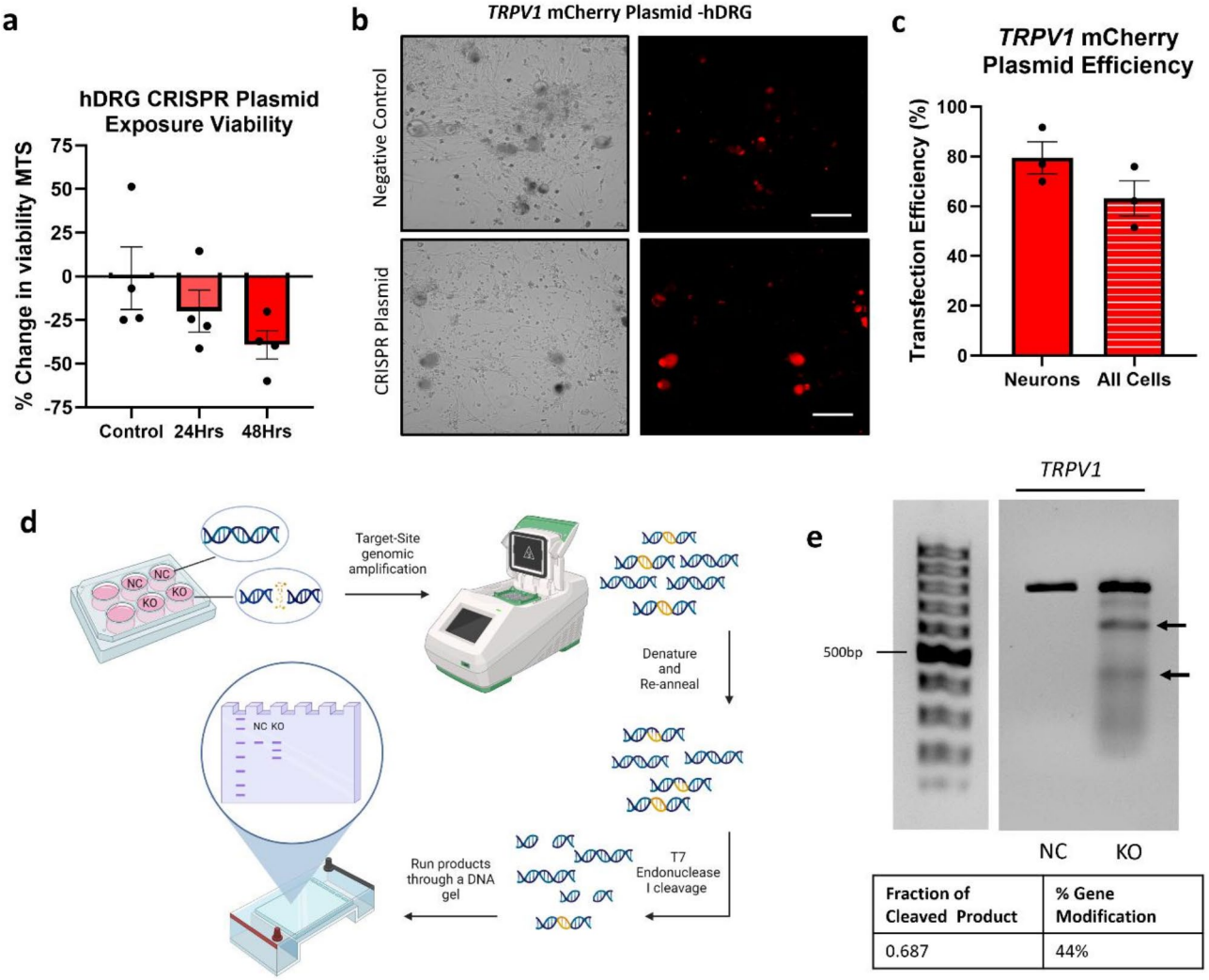

Fig. 2. Validation of CRISPR-Cas9 transfection with reporter tag and T7 endonuclease assay. **a.** MTS % change in viability in hDRG cultured cells treated for either 24- or 48 - hours with the *TRPV1* gRNA plasmid (500ng) demonstrating cells should not be exposed to the lipid-plasmid complex for more than 24-hours. There were no statistically significant differences between any of the groups using a one-way ANOVA using Tukey's multiple comparison test **b**. Fluorescent live images of mCherry reporter tag expression in the CRISPR-Cas9 *TRPV1* KO plasmid treated cells (bottom), compared to the negative control cells (top). Representative brightfield images (left) and the fluorescent images (right) were taken using a Biorad ZOE Fluorescent cell imager. Scale bar 100 µm **c**. % transfection efficiency for the *TRPV1* CRISPR plasmid quantified by fluorescent tag expression in neurons alone (77%) and in the entire hDRG culture (63%). Each point represents the average of at least 100 neuronal and at least 600 non-neuronal cells quantified from 3 individual replicates. The transfection efficiency denoted as all cells includes both neuronal and non-neuronal cells. **d**. Visual workflow of T7 endonuclease I assay used to confirm CRISPR-Cas9 genetic edit. **e.** Representative image of DNA gel demonstrating multiple DNA band fragments in the *TRPV1* CRISPR Plasmid exposed sample compared to the single negative control sample band (original gel in supplementary Fig. 2). Quantification of the bands was done through ImageJ to obtain the fraction of cleaved PCR products and the % of gene edit modification.

enzyme cleaved the DNA of the cells exposed to the *TRPV1* CRISPR plasmid but not the negative control cell's DNA (Fig. 2e). We also quantified the fraction of cleaved PCR product using the previously published formula (0.69) and then calculated the percent gene modification which came out to be 44%[39]. This confirmed successful DNA editing of the *TRPV1* gene in CRISPR treated hDRG cultures.

Changes in protein expression of CRISPR-Cas9 treated hDRG neurons

To further validate specific editing of the target gene, *TRPV1*, we performed immunocytochemistry (ICC) and western blotting to assess changes in protein expression in the hDRG cultures. Five days post transfection, we fixed cells on cover slips for ICC and collected whole cell lysates from 6-well plates for Western Blot quantification of TRPV1 protein expression. We chose peripherin, an intermediate filament enriched in peripheral neurons[40]and

expressed by all hDRG neurons[41], to label neurons in ICC coverslips. When compared to the negative control cells, TRPV1 expression was significantly decreased; Showing a 70% reduction in fluorescent intensity of TRPV1 protein expression in neurons labeled by peripherin (Fig. 3a.**b**). Moreover, the mCherry reporter tag was still expressed five days post transfection (Fig. 3a). We quantified the total change of TRPV1 expression in the whole lysates of hDRG culture by Western Blot, which demonstrated a statistically significant 50% decrease in TRPV1 expression (Fig. 3c). Overall, this data demonstrates successful editing and reduced TRPV1 protein expression in hDRG culture.

TRPV1 functional expression is decreased after CRISPR-Cas9 knockout in hDRG neurons

To demonstrate a decrease in protein function in response to the TRPV1 knockout we utilized a fluorescent imaging plate reader to detect changes in intracellular Ca^{2+} levels. Using Fura 2 AM dye we quantified the 340/380 ratio in response to capsaicin, an established specific TRPV1 agonist, or vehicle. The cells were seeded into a 96-well plate and transfected 24-hours later with 500 ng of CRISPR plasmid plus lipofectamine. Negative control wells received only lipofectamine treatment with the same timeline as the DNA-lipid complex treated wells. Three days post transfection the cells were incubated with Fura-2 AM/Pluronic F-127 (1:1) in Tyrode's buffer

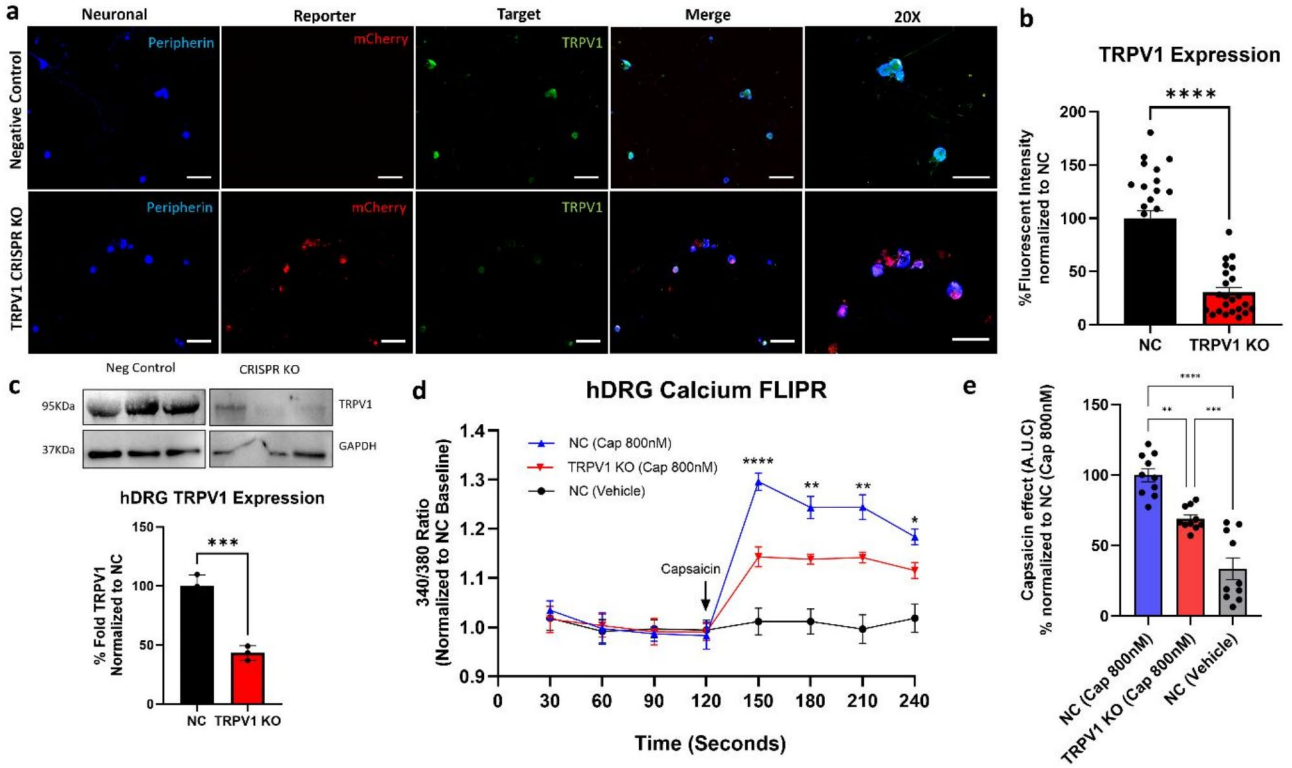

Fig. 3. Validation of decreased protein expression and protein function in *TRPV1* CRISPR cells. hDRG cells were transfected with CRISPR-Cas9 plasmid targeting *TRPV1* and were either fixed or lysed for protein 5-days later and analyzed via western blot or immunocytochemistry. **(a)** Representative 10X fluorescent images of TRPV1 in NC or CRISPR-Cas9 treated cells. Peripherin (blue) marked neurons, mCherry was seen only in the CRISPR-treated cells, and TRPV1 is significantly decreased these cells. The merge images of all three channels are shown for each negative control and CRISPR treated cells with the corresponding 20X image. **(b)** Data for the mean fluorescent intensity of TRPV1 (Green) was quantified as means ± SEM of $n = 10$ neurons per group in 3 individual replicates normalized to NC control average (100%). ****$P < 0.0001$ by unpaired two-tailed t-test. Scale bars = 100 µm **(c)** The representative Western blot and quantification of TRPV1; data was normalized to total protein, then further normalized to the negative control group (100%) (original blot in supplementary Fig. 2). ** = $p < 0.01$ by unpaired two-tailed t-test. **(d)** 72-hours post-transfection, the cells were incubated with Tyrode's buffer containing 2 µm Fura 2-AM/ Pluronic F-127 covered at room temperature for an hour then incubated with Tyrode's buffer supplemented with 2.5 mM probenecid for 20–30 min. A 2-minute baseline was recorded followed by 800nM capsaicin stimulation recorded for 2-minutes in 30 s intervals. A decreased capsaicin evoked calcium response is seen in the TRPV1-CRISPR-KO cells compared to the NC capsaicin cells. The data was reported as the 340/380 ratio and normalized to a 4-point negative control baseline. NC-Capsaicin vs. NC vehicle same time point; **** = $p < 0.0001$; ** = $p < 0.01$; * = $p < 0.05$;2-Way ANOVA with Tukey's post hoc test. Data was measured in two separate donors with 4–6 individual replicates per group. **(e)** Representative area under the curve (AUC) comparing vehicle, NC (Cap 800nM), and TRPV1 KO (800nM) capsaicin response post 120 s timepoint; data normalized to NC (cap 800nM) (100%). **** = $p < 0.0001$; *** = $p < 0.001$; ** = $p < 0.01$ by ordinary one-way ANOVA with Tukey's multiple comparison test.

for one hour at room temperature, followed by 30-minute incubation with Tyrode's with 2.5 mM probenecid to improve intracellular indicator retention. To assess functional knockout of *TRPV1*, we recorded a 2-minute baseline and proceeded to stimulate the cells with 800 nM capsaicin. We recorded the fluorescent intensity for 2-minutes post stimulation in 30-second intervals. Compared to the negative control wells, the *TRPV1*-edited wells had a significantly reduced response to 800nM capsaicin; The cells exposed only to vehicle showed no change in their intracellular Ca^{2+} concentration (Fig. 3d) and the AUC is a direct quantitative measure of the responses depicted by capturing the cumulative capsaicin effect over time. (Fig. 3e). We conclude CRISPR-Cas9 editing of the *TRPV1* gene in hDRG culture results in decrease of functional receptor activity 3 days post transfection.

CRISPR-Cas9 genetic editing of *NTSR2* and *CACNA1E* in hDRG cultures

We selected two other targets for editing, the G-protein coupled receptor (GPCR) neurotensin receptor 2 *(NTSR2*), and the R-type voltage gated calcium channel Cav2.3 (*CACNA1E*). These plasmids were also designed to contain a U6 promoter followed by a single guide RNA for the target of interest with the Cas9 being driven by a CMV promoter, but instead of mCherry, we chose GFP as the reporter tag (Fig. 1d). Like the mCherry plasmid, the expression of the GFP tag began 2 days post-transfection and both *CACNA1E* and *NTSR2* gRNA transfected cells showed robust expression of the GFP reporter tag compared to the negative control cells: showing an approximate 50% and 60% respective transfection efficiency (Fig. 4a-c). To determine if there were differences in viability between the cells treated with the three different CRISPR plasmids or their respective tags, we performed an ATP luminescent assay. Compared to the control non-CRISPR-treated cells, the cells exposed to the GFP lipid-plasmids displayed a statistically significant decrease in viability, but there were no statistically significant differences between the control cells and the *TRPV1* CRISPR plasmid transfected cell (Fig. 4d). It is important to note, there were no statistically significant differences between the control cells and the cells treated with Lipofectmaine3000 alone, or Lipofectamine3000 treatment compared to the DNA-lipid treated cultures. Overall, the cells exposed to the plasmid containing the mCherry tag were easier to confirm transfection as we could better differentiate between the lipofuscin and the fluorescent tag (Fig. 2b). This led us to conclude that the plasmid containing the mCherry reporter tag may be preferential for future experiments to ensure better visualization of expression.

We validated the genetic editing of these targets (*NTSR2* & *CACNA1E)* using the T7 endonuclease method as with the *TRPV1* plasmid (Fig. 4e). Similarly, we calculated the fraction of cleaved PCR product (0.71 & 0.72), as well as the percent of gene editing (46.3% & 47%) for CACNA1E and NTSR2 respectively (Fig. 4e). We observed a significant reduction in protein expression via Western blot with a 62% reduction in Cav2.3 and a 63% reduction in NTSR2 expression in culture (Fig. 4f, g**).** There was also a significant reduction of fluorescent intensity representative of Cav2.3 and NTSR2 in peripherin positive neurons, and the reporter tag was still expressed five days out from transfection (Fig. 5a, b). Therefore, we have validated the transfection method for two additional targets: one a GPCR and the other a voltage-gated ion channel.

Discussion

In summary, we provide a non-viral lipid-based transfection method to perform CRISPR-Cas9 genomic edits in primary human DRG culture. Primary neuronal cultures are difficult to maintain, and several factors such as culturing conditions, donor age, and postmortem interval can affect the overall health of the culture[42]. The primary culture method developed by our group was described in Supplemental Fig. 1 and is a key component to maintaining a healthy DRG neuronal culture. The postmortem interval for all the donors was less than four hours, which is another key factor influencing culture viability and high cell yield. We also observed hDRG cultures from older aged donors typically showed lower neuronal cell yields and subsequently lower viability when subjected to lipofectamine transfection leading to cell loss in an already depleted neuronal population. For most of the experiments, we preferentially used DRGs recovered from donors not exceeding 50 years of age (Fig. 1b) (Supplementary Table 1).

The transfection efficiency can depend on the promoters used, we chose plasmids containing the universal U6 promoter driving the sgRNA sequence, and the non-specific CMV promoter driving the Cas9 protein (Fig. 1d)[43]. The plasmids also contained a reporter tag (GFP or mCherry) and a neomycin resistance gene for mammalian cell selection. Our initial step to verify if we achieved transfection was fluorescent live cell imaging to observe the expression of the reporter tags (GFP or mCherry). The robust expression of the reporter tags in neurons demonstrated the lipofectamine as an efficient delivery method, and the promoters are sufficient at driving expression to cause genetic editing. Out of the three CRISPR plasmid constructs tested, the minimum transfection efficiency was 50% for the *CACNA1E* construct (Fig. 4b). The lipid-plasmid complex should not be left in the culture media for more than 24-h. This is in part due to the change in viability, but also because the lipid-plasmids complexes can lower the pH of the culture medium, and this in turn can affect the fluorescent intensity of the reporter tags (Fig. 2a)[44]. Lipofectamine, as a delivery system, is known to exhibit some degree of cytotoxicity across various tissue types[45]. To specifically evaluate its effect on primary human sensory neurons, we assessed cell viability at 24- and 48-hour exposure periods (Fig. 2a). The apparent reduction in cell viability reflects our intention to establish the upper threshold of toxicity under these conditions. When the complex is removed after 24-h, as per our optimized protocol, there is a moderate, expected reduction in viability (~10–25%). This effect stabilizes over subsequent days, with no significant increase in cell death observed. Our day 3 post-transfection cell viability assay further confirms this (Fig. 4d), showing approximately 30% viability reduction in one CRISPR plasmid group compared to the non-transfected control. For future studies, it is possible to design the plasmid to contain a cell specific promoter to drive the Cas9 protein, and therefore lead to a targeted knockout in a cell specific manner[46]. FACS sorting the cells using the reporter tag leads to an enriched transfected cell population, but due to the large diameter size and the fragility of the hDRG neurons, this was not

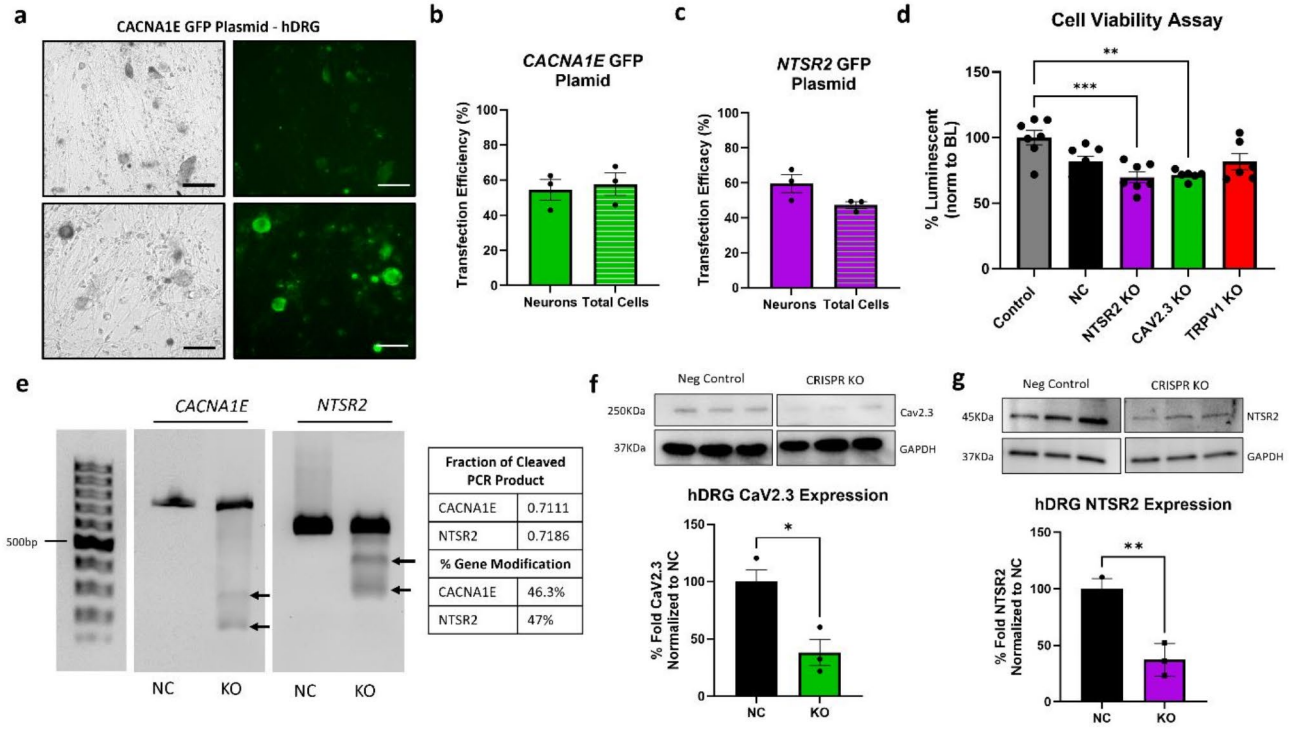

Fig. 4. CRISPR-Cas9 genetic editing of *NTSR2* and *CACNA1E* in hDRG cultures. **a.** Representative fluorescent live cell images of GFP reporter tag expression in the CRISPR-Cas9 *CACNA1E* KO plasmid treated cells (bottom), compared to the negative control cells (top). Representative brightfield images (left) and the fluorescent images (right) were taken using a Biorad ZOE Fluorescent cell imager. Scale bar 100 µm. **b.** Percent transfection efficiency for the *CACNA1E* CRISPR plasmid quantified by fluorescent tag expression in neurons alone and in the entire hDRG culture. **c.** Percent transfection efficiency for the *NTSR2* CRISPR plasmid quantified by fluorescent tag expression in neurons alone and in the entire hDRG culture. (Images not shown). Each point represents the average of at least 100 neuronal and at least 600 non-neuronal cells quantified from 3-individual replicates. The transfection efficiency denoted as all cells includes both neuronal and non-neuronal cells. **d.** CellTiter Glo 2.0 Assay demonstrating viability of cells may differ between the cells exposed to plasmids containing the GFP compared to the mCherry reporter. Both *NTSR2* and *CACNA1E* DNA plasmids with GFP reporter tags show a significant decrease in viability compared to non-treated control cells but not in comparison to lipofectamine treated NC cells. Both lipofectamine alone and the mCherry tag plasmid (*TRPV1*) show no significant decrease in viability compared to the non-treated control cells. Luminescence was measured across two different donors with 3 individual replicates per treatment group using a Tecan Spark 20 plate reader; *** = $p < 0.001$; ** = $p < 0.01$; by 1-Way ANOVA with Tukey's post-hoc test **e.** Representative image of DNA gel demonstrating multiple DNA band fragments in the *NTSR2 & CACNA1E* CRISPR plasmid exposed sample compared to the single negative control sample band. **f**. Representative Western blot and quantification of NTSR2; data was normalized to GAPDH, then normalized to the negative control group (100%). ** = $p < 0.01$; * = $p < 0.1$ by unpaired 2-tailed t-test. **g.** Representative Western blot and quantification of Cav2.3; data was normalized to GAPDH, then normalized to the negative control group (100%). * = $p < 0.05$ by unpaired 2-tailed t-test. (original gel and blots in supplementary Fig. 2).

a practical option. In addition, we chose not to use neomycin to preferentially select transfected cells as it can be toxic to mammalian cells, and we did not want to further risk the viability of hDRG cultures[47].

A CRISPR genomic edit can be confirmed using Sanger DNA sequencing or tracking of indels by decomposition (TIDE) assay, however we chose a simpler more time efficient method by using an indel assay with enzymatic digestion that can be performed 36–48 h post transfection (Fig. 2d). This assay confirmed genetic editing in culture, specifically in the targeted gene regions of interest (*CACNA1E*, *TRPV1*, *NTRS2*) (Figs. 2 and 4). Confirmation of significant protein changes in the entire culture were seen via western blots with a 57% (TRPV1), 62% (CAV2.3) and a 64% (NTSR2) (Figs. 3, 4 and 5). Likewise, significant protein changes were observed specifically in the peripherin-positive neuronal population through immunocytochemistry, with a reduction in fluorescent intensity of 70% (TRPV1), 63% (CAV2.3) and 75% (NTSR2) (Figs. 3 and 5). It is important to note this is a primary mixed culture, the western blot results represent the expression levels of the target proteins across several different cell types. In contrast, the immunocytochemistry results are specific to the neuronal population, reflecting protein expression only in neurons, this could explain why the knockout efficiency differs slightly between the two. Similarly, the transfection efficiency primarily indicates the proportion of cells that have successfully taken up the CRISPR plasmids. However, this metric does not necessarily correlate

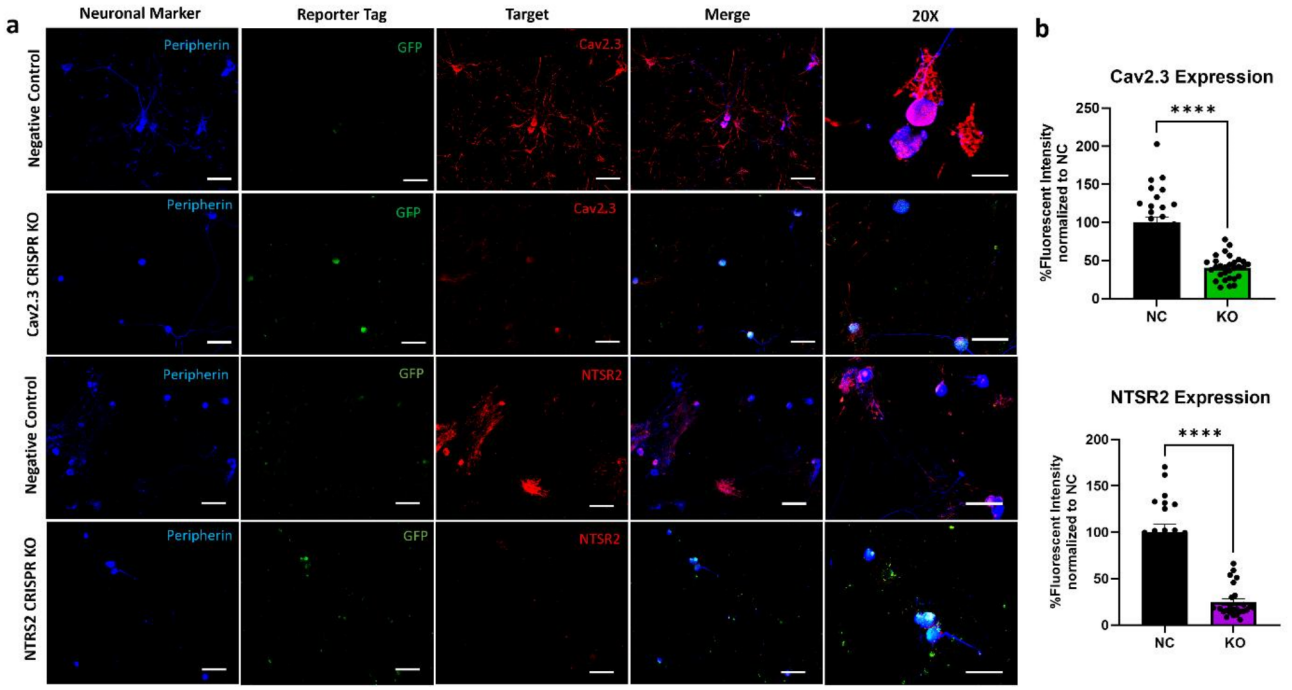

Fig. 5. Immunocytochemistry validation of CRISPR editing of NTSR2 and Cav2.3 protein levels in hDRG culture. Representative 10X fluorescent images staining for NTSR2 and Cav2.3 of negative control or CRISPR-Cas9 treated hDRG cultures. **(a)** Peripherin (blue) was used as the neuronal marker, the reporter tag (GFP) was seen only in the CRISPR treated cells, while the target of interest is significantly decreased in the perspective CRISPR treated cells. The merge images of all three channels are shown for each negative control and CRISPR treated cells with the corresponding 20X image. **(b)** Data for the mean fluorescent intensity for the targets of interest Cav2.3 (Red), and NTSR2 (Red) was quantified as means ± SEM of $n = 10$ neurons per group in 3 individual replicates; data normalized to NC control (100%).$^{****}P < 0.0001$ by unpaired two-tailed t-test. Scale bars = 100 µm.

with editing efficiency, which may be lower. Together, we conclude achievement of high delivery efficiency of the CRISPR plasmids for our three targets of interest; Cav2.3, NTSR2, & TRPV1.

To test the effect of the knockout on protein function, we developed a protocol for measuring intracellular Ca^{+2} by using a fluorescent imaging plate reader (FLIPR) assay with the calcium indicator Fura 2AM dye in primary hDRG culture, a method which can be used in a high through put screening (HTS) fashion (Fig. 3)[48,49]. A FLIPR is a very efficient tool at detecting comprehensive and homogenous intracellular Ca^{+2}changes and has shown promise as a functional output in human iPSC-derived nociceptors (hiPSCdNC)[50,51]. TRPV1 edited wells showed a significant decrease in response to capsaicin compared to negative control wells; However, it did not abolish it completely as compared to non-stimulated cells (Fig. 3). This could be due to residual TRPV1 channel protein reserve present in the cells, as the experiment was performed on the 3rd day post transfection. If we maintained the cells on these plates 5 days post transfection, we may have seen a greater decrease in functional TRPV1. However, the small surface area in the 96-well plate becomes a limiting factor for how many days the cells can be maintained in culture before overgrowth of glial cells overcrowd neurons. Some compromises between the type of primary culture and the degree to which editing will be reflected in protein turnover need to be considered in experimental design.

The advancement of nano-delivery systems has been beneficial in providing easy to use, reliable transfection of nucleic acids into target cells[52,53]. With the growing application of genomic engineering in the clinic, cationic lipid nanoparticles are more likely to have a greater impact over viral vectors. To our knowledge, we demonstrated the first successful lipid-based delivery method of CRISPR-Cas9 genome editing system in primary human DRG neurons. Overall, our work provides evidence that a cationic lipid delivery system is a viable transfection method for gene editing in primary human neurons which can be utilized in many cell-based assays. In summary, we provide a straightforward method for genome editing in human DRG neurons which will enable precise dissection of mechanisms in these cells and enables future work for therapeutic application.

Materials and methods

Human DRG collection

All human tissue procurement procedures were approved by the Institutional Review Boards at the University of Texas at Dallas. All experiments were performed in accordance with relevant guidelines and regulations of the Institutional Review Boards. Human DRGs were surgically extracted using a ventral approach[54] from organ donors within 4 h of cross-clamp and placed immediately on artificial cerebrospinal fluid (aCSF). All tissues

were recovered in the Dallas area via a collaboration with the Southwest Transplant Alliance. Tissue samples from 12 donors were used in this study, information is provided in Table 1.

Human DRG dissociation protocol

The recovered DRG was trimmed with No. 5 forceps (Fine Science Tools, Cat#11252-00) and Bonn scissors (Fine Science Tools, Cat# 14184-09) to expose the cluster of cell bodies. At the time of culturing, a final enzyme solution consisting of 2 mg/mL Stemzyme I (Worthington Biochemical, Cat#LS004106) and 0.1 mg/mL DNAse I was prepared in HBSS (Thermo Scientific, Cat#14170161) and allowed to incubate in a water bath. A total of 5 mL of enzyme solution was used to dissociate the hDRG tissue. Ganglia were finely minced with scissors into smaller fragments less than 3 mm (about 0.12 in). The tissue fragments were transferred to the prewarmed enzyme solutions in 10 mL conical tubes and placed in a 37 °C shaking water bath until the tissue completely dissociated resulting in a cloudy solution (6–18 h in total). The solution containing dissociated neurons was passed through a 100 µm sterile cell strainer (VWR, Cat# 21008-950) into a 50 mL conical tube. The cell suspension was then gently added to a 3 mL 10% Bovine Serum Albumin (Biopharm, Cat#71040)/HBSS gradient and spun down at 900*xg* for 5 min at RTP, 9 acceleration, 5 deceleration. The resulting pallet of cells at the bottom of the tube was resuspended in prewarmed and sterile filtered DRG media. 20µL of cell suspension was carefully plated onto the 96-well plate, 120µL onto each coverslip, and 500µL onto the 6 well plates at a density of at least 150, 300, and 800 neurons respectively, and allowed to adhere for 3 h at 37 °C and 5% CO2. The wells were flooded with the appropriate amount depending on the plate of prewarmed complete hDRG media. Media changes were performed every other day. Primary hDRG neurons are non-dividing postmitotic cells that are difficult to maintain; therefore, to achieve the most optimal cell count and cell health for the transfection experiments, donors above 50 years old were excluded.

Antibodies

Antibodies used were as follows: Peripherin (chicken 1:1000; EnCor, AB_2284443) Cav2.3 (Rabbit, Alomone labs, 1:100 AB_2039777; lot ACC006AN0302), NTSR2 (rabbit, 1:200, ThermoFisher BS-12004R), TRPV1 (Rabbit, 1:500 Fisher scientific PA1748) GAPDH (mouse, Cell signaling 97166s) secondary Alexa Fluor goat anti-mouse immunoglobulin G (IgG) 594 (1:5000; Invitrogen, A11032, lot 1985396), and secondary Alexa Fluor goat anti-mouse IgG 488 (1:5000; Invitrogen A-11034, lot 2110499). Alexa Fluor goat anti-chicken IgG 647 (1:5000; Invitrogen A-21449, lot 2186435).

Plating media

BrainPhys® media (Stemcell technologies, cat. no. 05790), 1% penicillin/streptomycin (Thermo Fisher Scientific, Cat# 15070063), 1% GlutaMAX® (United States Biological, cat. no. 235242), 2% NeuroCult™ SM1 (Stemcell technologies, cat. no. 05711), 1% N-2 Supplement (Thermo Scientific, cat. no. 17502048), 2% HyClone™ Fetal Bovine Serum (ThermoFisher Scientific SH3008803IR), 1: 1000 FrdU, 10 ng/mL Human β nerve growth factor - (Cell Signaling Technology, Cat# 5221SC).

CRISPR construct

The custom CRISPR gene editing constructs were obtained from Genecopoeia as an all-in-one CRISPR clone with a single guide RNA (sgRNA) targeting all variants for *CACNA1E* (target Site: CCTCAGGATGGCTCGC TTCG), *NTSR2* (target site: CCGCGCTCTACGCACTCATC), *TRPV1* (target site: CCCGGTGGATTGCCCT CACG) and the Cas9 gene, along with a neomycin resistance gene for mammalian cell selection and either an mCherry or GFP gene for visualization. (no. HCP001992-CG04-1B, HCP206276-CG04-1-B, HCP002057-CG12-1-B respectively). After the Cas9 sequence the plasmid carrying an mCherry reporter tag expresses downstream from an EF1a promoter while the GFP tag expresses downstream from T2A spacer sequence (Fig. 2B). Also included in the plasmids is a neomycin resistance gene for mammalian cell selection. Each DNA vector was amplified for use using standard bacterial transformation and an endotoxin-free maxi-prep Qiagen kit.

Transfection efficiency quantification

Live cell images were obtained using a Biorad ZOE Fluorescent cell imager. Four fields of view were obtained and quantified from each individual well, with each condition having 3 individual replicates. Images were acquired in both brightfield and TRITC channel for all four fields of view. The percent transfection efficiency for all three CRISPR plasmids was quantified by counting all the cells in each individual field of view per well in the brightfield images first. The neurons were also counted alone, which are easily distinguished by their circular structure, the large diameter and presence of lipofuscin. Then we moved on to quantifying each fluorescent cell in the TRITC channel. Satellite glial cells and immune cells, which are present in the primary culture and much smaller than neurons, do not autofluorescence unless they have been transfected and were easily identified. Cross referencing the dark pigment in the brightfield images, the lipofuscin was marked and not used to count the fluorescence. For each individual replicate, we quantified an average of at least 100 neurons, and at least 600 non-neuronal cells. The number of fluorescent cells was divided by the total number of cells in the field and multiplied by 100 to obtain a percent of transfection.

Western blotting and analysis

Human DRG protein lysates were collected in ice cold lysis buffer (20 mM Tris-HCl (pH 7.4), 50 mM NaCl, 2 mM $MgCl_2$ hexahydrate, 1% (*v*/*v*) NP40, 0.5% (*w*/*v*) sodium deoxycholate, 0.1% (*w*/*v*) SDS supplemented with protease and phosphatase inhibitor cocktail (BiMake)). The tissue lysate was centrifuged at 12,000× *g* for 10 min at 4 °C, then the supernatant was collected and used for determination of protein content with a BCA assay. Total protein (20–40 µg) from tissue supernatant was loaded into TGX precast gels (4–20% CriterionTM, BioRad)

and transferred to nitrocellulose membrane (AmershamTM ProtranTM, GE Healthcare). After transfer, the membrane was blocked at room temperature for 1 h in blocking buffer (5% dry milk in Tris-buffered saline with tween 20 (TBST)). The membrane was incubated in diluted primary antibodies for 24 h at 4 °C. The membrane was washed three times in TBST for 5 min each then incubated with peroxidase-conjugated secondary antibodies for one hour rocking at room temperature. The membrane was then washed in TBST for 5 min each and then incubated with BioRad clarity western ECL substrate and Millipore HRP substrate solutions and then imaged in a ChemiDoc MP from BioRad. Some blots were then stripped with 25 mM glycine-HCl and 1% SDS (pH 2.0) for 30 to 60 min of rocking at room temperature before being washed and re-exposed to primary antibody. The resulting image bands were quantified using Scion Image (based on NIH Image). All images were quantified in the linear signal range. The intensities were normalized to GAPDH for Cav2.3, and for NTSR2 and TRPV1, the data was normalized to total protein. The normalized intensities were further normalized to a negative CRISPR control present on the same blot.

Immunocytochemistry

The treated cultures were immediately fixed with 10% formalin (ThermoFisher Scientific, Cat# 23–245684) for 15 min at room temperature and rinsed three times with 1X PBS. 1 h block was performed at room temperature with 10% NGS and 0.3% Triton X-100 in 1X PBS. The coverslips were then incubated overnight at 4 °C with primary antibodies anti-peripherin (chicken 1:1000; EnCor, AB_2284443) Cav2.3 (rabbit, Alomone labs, 1:100 AB_2039777; lot ACC006AN0302), NTSR2 (rabbit, 1:200, Thermo Fisher BS-12004R), TRPV1 (Rabbit, 1:500 Fisher scientific PA1748). Coverslips were rinsed 3 times with 1X PBS for 15 min and incubated with secondary antibodies Alexa Fluor goat anti-chicken IgG 647 (1:5000; Invitrogen A-21449, lot 2186435), Alexa Fluor goat anti-rabbit IgG 488 (1:5000; Invitrogen A-11034, lot 2110499) and Alexa Fluor goat anti-mouse IgG 594 (1:5000; Invitrogen, A11032, lot 1985396) for 1 h at room temperature. The coverslips were washed 3 times with 1X PBS and mounted with prolong gold onto uncharged glass slides and allowed to cure overnight. Slides were imaged at 10X and 20X magnification using the Olympus FV1200 RS confocal laser scanning microscope.

CRISPR insertion or deletion detection system with T7 endonuclease I

36–48 hours post transfection of CRISPR plasmid constructs into cultured primary Human DRG the 6-well plate was removed from the incubator, media removed, and cells rinsed with 1 mL of PBS twice. Whole cell lysate preparation of primary cultured Human Dorsal Root Ganglia was collected by adding 200–300 uL of lysis buffer, provided in IndelCheck™ kit purchased from GeneCopoeia (Cat# IC001), into each well followed by use of a cell scrapper. Lysates were briefly vortexed before heating samples at 65ºC for 20min, then 95ºC for 10 min in a heat block. Lysates were quickly placed in ice for 1 minute before centrifugation at 12,000 RPM for 1 minute, supernatant of each sample was collected and placed in separate tube. Samples were then subjected to standard PCR. The 2x superhero PCR mix provided in the IndelCheck kit was used with primers purchased from GeneCopoeia specific to each target. Target site PCR primer for indel detection for NTSR2; Cat# HCP206276-CG04-1-B (NM_012344.3) (forward sequence: 5'- CGGTCCCACGTTGGCTCAGG – 3' and reverse sequence: 5'- ACCAGCACCGTGCACACTCG – 3'); Target site PCR primer for indel detection for CaV2.3; Cat# HCP001992-CG04-1-B (Gene ID: 777), (forward sequence: 5'- CTGGGCACCCCCAAGCCCTA – 3'; reverse sequence: 5'- CCCAAACGGGTCTCCACGGC – 3') and TRPV1; Cat# PHCP002057-a (Gene ID: 7442), (forward sequence: 5'- TTTCCTTGTTCTGTGTGGGG – 3; reverse sequence: 5'-GACATTTAGCCCA GAAGCCA – 3'). 8 uL of lysate was mixed with 1.25 uL of forward and reverse primers (5 µm each) 12.5 uL 2xsuperhero PCR mix and 3.25 uL of nuclease free water for a total of 25 uL per sample. Samples placed into PCR tubes and put into Biorad thermocycler using the following settings: 94ºC 5 min for 1 cycle; followed by 30 cycles at 94ºC 30 s; 58ºC for 30 s; 72ºC for 1 min; and finally, 1 cycle at 72ºC for 5 min. For the denaturing and annealing process, 10 uL of each sample PCR product was mixed with 9 uL of nuclease free water for a total volume of 19 uL. Each mixture was mixed and centrifugated in a benchtop mini centrifuge for 30 s. Samples were placed in heat block set at 95ºC for 5 min followed by a reannealing period at room temperature for 5–10 min. 1 uL of T7 endonuclease provided in kit was added to each sample and incubated at 37ºC for 45–60 min. Samples were prepared with loading buffer and gel green to be loaded into wells of a 1.5% agarose DNA gel along with DNA ladder. Gel was run at 90 V in TBE. Afterward, the gel was imaged using Biorad ChemiDoc Touch Imaging System imager. The fraction of cleaved PCR product was calculated using the previously published formula f(cut) = a/a + b where a is the integrated intensity of both cleavage product bands and b = the integrated intensity of uncleaved PCR product band[39].

Fluorescent imaging plate reader-based calcium assay

Human dorsal root ganglion (hDRG) was collected from donor and subjected to above listed primary culture protocols and seeded into a clear flat-bottom black 96-well culture plate (Corning Inc 3603) coated with 100 µg/mL PDL. The cells were maintained at 37ºC, 5% CO2 for 24 h. After 24 h the cells were transfected with CRISPR/Cas-9 construct using lipofectamine 3000 (ThermoFisher L3000015) and were left in the incubator for 18–24 h at 37ºC, 5% CO2. Seetable 1for DNA/lipofectamine 3000 lipid complex ratio used. The media containing lipid/DNA complex was replaced with regular hDRG media after 18–24-hour incubation. 48-hours after media replacement the plate was pulled from the incubator and media removed from the wells, each well was washed once with 200uL of Tyrode's buffer (NaCl 119 mM, KCl 2.5 mM, MgCl2 2 mM, CaCl2 2 mM, HEPES 25 mM, Glucose 30 mM). Following wash, 150uL of Tyrode's containing 2 µm Fura 2-AM (Invitrogen F1221, Lot 2559176)/ Pluronic F-127 (Invitrogen P3000MP, lot 2510678) (mixed 1:1 by volume) was added to each well containing cells. The plate was incubated while covered at room temperature for an hour. The dye solution was removed, the wells were washed twice with Tyrode's buffer before adding 150uL of Tyrode's buffer supplemented with 2.5 mM probenecid (Invitrogen P36400, lot 2600149), left to rest covered at room temperature for 20–30 min, followed

by an extra wash with Tyrode's buffer supplement with probenecid. After incubation period, the plate was placed into Tecan plate reading instrument for five time point baseline. Plate was removed and media replaced. The NC and KO wells received 150 uL of Tyrode's supplemented with probenecid with 800 nM capsaicin (Sigma M2028-50MG, Lot SLCB0726) while the non-stimulated control well received only Tyrode's supplemented with probenecid. The plate was placed back into the instrument and 12 points were read post capsaicin treatment. Each read point was 30 s apart. See Supplementary Table 2 for instrument reader parameters.

Viability assays

Two different viability dyes were utilized in the experiments: CellTiter Glo 2.0 and the CellTiter 96 Aqueaous one solution cell proliferation assay (MTS). For both assays we chose to use a 96-well plate and seeded the hDRG cultures at a density of at least 150 neurons per well. For the MTS assay, we preincubated 20ul of the dye per 100ul of media for 2 h at 37ºC, 5% CO2, and recorded the absorbance at 490 nm. Media was completely changed, and the cells were either transfected with the *TRPV1* gRNA plasmid, lipofectamine without plasmid, or just media for 24 h at 37ºC, 5% CO2. Media was changed and 20ul of the MTS dye was added to the cells per 100ul of media and absorbance was recorded two hours later at 490 nm. The percent change in viability was determined using the following equation ((post-treatment MTS – Pre-treatment MTS)/Average Pre-treatment MTS)) *100[55]. For the CellTiter Glo 2.0, we added 1:1 ratio of media to dye to the wells post treatment with either the *TRPV1*, *CACNA1E*, *NTSR2* gRNA plasmid (500ng), lipofectamine alone, or media alone. The plate was placed in an orbital shaker at room temp for 2 min to induce cell lysis and luminescence was recorded 10 min later. Both assays were recorded using a Tecan Spark 20 plate reader.

Data availability

All data is provided within the main text or supplementary information files. The tissues obtained were donated by organ donors to Southwest Transplant Alliance. Southwest Transplant Alliance received informed consent agreements provided legally from next of kin, who consented to their family members' tissues being utilized for research purposes.

Received: 4 October 2024; Accepted: 18 February 2025
Published online: 01 April 2025

References

1. Doudna, J. A. & Charpentier, E. Genome editing. The new frontier of genome engineering with CRISPR-Cas9. *Science* **346**, 1258096 (2014).
2. Jiang, F. & Doudna, J. A. CRISPR-Cas9 structures and mechanisms. *Annu. Rev. Biophys.* **46**, 505–529 (2017).
3. Ovcharenko, D., Jarvis, R., Hunicke-Smith, S., Kelnar, K. & Brown, D. High-throughput RNAi screening in vitro: from cell lines to primary cells. *Rna* **11**, 985–993 (2005).
4. Hsu, S., Huang, G. S., Ho, T. T. & Feng, F. Efficient gene Silencing in mesenchymal stem cells by substrate-mediated RNA interference. *Tissue Eng. Part. C: Methods*. **20**, 916–930 (2014).
5. Barrangou, R. & Doudna, J. A. Applications of CRISPR technologies in research and beyond. *Nat. Biotechnol.* **34**, 933–941 (2016).
6. Fellmann, C., Gowen, B. G., Lin, P. C., Doudna, J. A. & Corn, J. E. Cornerstones of CRISPR-Cas in drug discovery and therapy. *Nat. Rev. Drug Discov*. **16**, 89–100 (2017).
7. Gaj, T., Sirk, S. J., Shui, S. & Liu, J. Genome-editing technologies: principles and applications. *Cold Spring Harb. Perspect. Biol.* **8**, a023754 (2016).
8. Wong, C. UK first to approve CRISPR treatment for diseases: what you need to know. *Nature* **623**, 676–677 (2023).
9. Hoy, S. M. Exagamglogene autotemcel: first approval. *Mol. Diagn. Ther.* **28**(2), 133–139 (2024).
10. Sharma, A. et al. CRISPR-Cas9 editing of the HBG1 and HBG2 promoters to treat sickle cell disease. *N. Engl. J. Med.* **389**, 820–832 (2023).
11. Bennet, B. M., Regulatory Policy Committee Technical Review. & et al Biology and pathology of ganglia in animal species used for nonclinical safety testing. *Toxicol. Pathol.* **51**, 278–305 (2023).
12. Buss, N. et al. Characterization of AAV-mediated dorsal root ganglionopathy. *Mol. Ther. Methods Clin. Dev.* **24**, 342–354 (2022).
13. Chen, X. et al. Intrathecal AAV9/AP4M1 gene therapy for hereditary spastic paraplegia 50 shows safety and efficacy in preclinical studies. *J. Clin. Invest.* **133**(10), e164575 (2023).
14. Hordeaux, J. et al. Adeno-Associated Virus-Induced dorsal root ganglion pathology. *Hum. Gene Ther.* **31**, 808–818 (2020).
15. Hordeaux, J. et al. MicroRNA-mediated inhibition of transgene expression reduces dorsal root ganglion toxicity by AAV vectors in primates. *Sci. Transl. Med.* **12**(569), eaba9188 (2020).
16. Chong, Z. X., Yeap, S. K. & Ho, W. Y. Transfection types, methods and strategies: A technical review. *PeerJ* **9**, e11165 (2021).
17. Gurumoorthy, N., Nordin, F., Tye, G. J., Wan Kamarul Zaman, W. S. & Ng, M. H. Non-integrating lentiviral vectors in clinical applications: A glance through. *Biomedicines* **10**, 107 (2022).
18. Felberbaum, R. S. The baculovirus expression vector system: A commercial manufacturing platform for viral vaccines and gene therapy vectors. *Biotechnol. J.* **10**, 702–714 (2015).
19. Hindriksen, S. et al. Baculoviral delivery of CRISPR/Cas9 facilitates efficient genome editing in human cells. *PloS One*. **12**, e0179514 (2017).
20. Kost, T. A., Condreay, J. P. & Jarvis, D. L. Baculovirus as versatile vectors for protein expression in insect and mammalian cells. *Nat. Biotechnol.* **23**, 567–575 (2005).
21. Mansouri, M. et al. Highly efficient baculovirus-mediated multigene delivery in primary cells. *Nat. Commun.* **7**, 11529 (2016).
22. Mansouri, M., Ehsaei, Z., Taylor, V. & Berger, P. Baculovirus-based genome editing in primary cells. *Plasmid* **90**, 5–9 (2017).
23. Moreno, A. M. et al. In situ gene therapy via AAV-CRISPR-Cas9-mediated targeted gene regulation. *Mol. Ther.* **26**, 1818–1827 (2018).
24. Senís, E. et al. CRISPR/Cas9-mediated genome engineering: an adeno-associated viral (AAV) vector toolbox. *Biotechnol. J.* **9**, 1402–1412 (2014).
25. Haberberger, R. V., Barry, C., Dominguez, N. & Matusica, D. Human dorsal root ganglia. *Front. Cell. Neurosci.* **13**, 271 (2019).
26. Pylaev, T., Vanzha, E., Avdeeva, E., Khlebtsov, B. & Khlebtsov, N. A novel cell transfection platform based on laser optoporation mediated by Au Nanostar layers. *J. Biophotonics*. **12**, e201800166 (2019).
27. Banskota, S. et al. Engineered virus-like particles for efficient in vivo delivery of therapeutic proteins. *Cell* **185**, 250–265 (2022).
28. Seow, Y. & Wood, M. J. Biological gene delivery vehicles: beyond viral vectors. *Mol. Ther.* **17**, 767–777 (2009).

29. Shalaby, K. E., Aouida, M., Gupta, V., Abdesselem, H. & El-Agnaf, O. M. Development of non-viral vectors for neuronal-targeted delivery of CRISPR-Cas9 RNA-proteins as a therapeutic strategy for neurological disorders. *Biomaterials Sci.* **10**, 4959–4977 (2022).
30. Matsuda, T. & Oinuma, I. Imaging endogenous synaptic proteins in primary neurons at single-cell resolution using CRISPR/Cas9. *Mol. Biol. Cell.* **30**, 2838–2855 (2019).
31. Thi, T. T. H. et al. Lipid-based nanoparticles in the clinic and clinical trials: from cancer nanomedicine to COVID-19 vaccines. *Vaccines* **9**, 359 (2021).
32. Sahin, U. et al. COVID-19 vaccine BNT162b1 elicits human antibody and T(H)1 T cell responses. *Nature* **586**, 594–599 (2020).
33. Li, Y. et al. MNK inhibitor eFT508 (Tomivosertib) suppresses ectopic activity in human dorsal root ganglion neurons from dermatomes with radicular neuropathic pain. *bioRxiv*, (2023).
34. Tavares-Ferreira, D. et al. Spatial transcriptomics of dorsal root ganglia identifies molecular signatures of human nociceptors. *Sci. Transl. Med.* **14**, eabj8186 (2022).
35. Caterina, M. J. et al. The capsaicin receptor: a heat-activated ion channel in the pain pathway. *Nature* **389**, 816–824 (1997).
36. Tominaga, M. et al. The cloned capsaicin receptor integrates multiple pain-producing stimuli. *Neuron* **21**, 531–543 (1998).
37. Yang, F. & Zheng, J. Understand spiciness: mechanism of TRPV1 channel activation by capsaicin. *Protein Cell.* **8**, 169–177 (2017).
38. Di Guardo, G. Lipofuscin, lipofuscin-like pigments and autofluorescence. *Eur. J. Histochemistry: EJH* **59**(1), 2485 (2015).
39. Sanjana, N. E. et al. A transcription activator-like effector toolbox for genome engineering. *Nat. Protoc.* **7**, 171–192 (2012).
40. Amaya, F. et al. Diversity of expression of the sensory neuron-specific TTX-resistant voltage-gated sodium ion channels SNS and SNS2. *Mol. Cell. Neurosci.* **15**, 331–342 (2000).
41. Shiers, S. I. et al. Convergence of peptidergic and non-peptidergic protein markers in the human dorsal root ganglion and spinal dorsal Horn. *J. Comp. Neurol.* **529**, 2771–2788 (2021).
42. Piwocka, O. et al. Navigating challenges: optimising methods for primary cell culture isolation. *Cancer Cell Int.* **24**, 28 (2024).
43. Ho, J. Y. et al. Promoter usage regulating the surface density of CAR molecules May modulate the kinetics of CAR-T cells in vivo. *Mol. Therapy-Methods Clin. Dev.* **21**, 237–246 (2021).
44. Doherty, G. P., Bailey, K. & Lewis, P. J. Stage-specific fluorescence intensity of GFP and mCherry during sporulation in Bacillus subtilis. *BMC Res. Notes.* **3**, 1–8 (2010).
45. Patil, S. D., Rhodes, D. G. & Burgess, D. J. Anionic liposomal delivery system for DNA transfection. *AAPS J.* **6**, 13–22 (2004).
46. Gabriel, K. A. & Streicher, J. M. HSP90 Inhibition in the mouse spinal cord enhances opioid signaling by suppressing an AMPK-mediated negative feedback loop. *Sci. Signal.* **16**, eade2438 (2023).
47. Kovacik, A. et al. Cytotoxic effect of aminoglycoside antibiotics on the mammalian cell lines. *J. Environ. Sci. Health Part. A.* **56**, 1–8 (2020).
48. Martínez, M., Martínez, N. A. & Silva, W. I. Measurement of the intracellular calcium concentration with Fura-2 AM using a fluorescence plate reader. *Bio-protocol* **7**, e2411–e2411 (2017).
49. Arkin, M. R. et al. FLIPR™ Assays for GPCR and Ion Channel Targets. *Assay Guidance Manual [Internet]*, (2012).
50. Röderer, P. et al. Emergence of nociceptive functionality and opioid signaling in human iPSC-derived sensory neurons. *Pain* **10**, 1097 (2022).
51. Zhang, Y. L. et al. Novel Fluorescence-Based High-Throughput FLIPR assay utilizing Membrane-Tethered genetic calcium sensors to identify T-Type calcium channel modulators. *ACS Pharmacol. Translational Sci.* **5**, 156–168 (2022).
52. Kim, T. K. & Eberwine, J. H. Mammalian cell transfection: the present and the future. *Anal. Bioanal. Chem.* **397**, 3173–3178 (2010).
53. Sahin, U., Kariko, K. & Tureci, O. mRNA-based therapeutics–developing a new class of drugs. *Nat. Rev. Drug Discov.* **13**, 759–780 (2014).
54. Valtcheva, M. V. et al. Surgical extraction of human dorsal root ganglia from organ donors and Preparation of primary sensory neuron cultures. *Nat. Protoc.* **11**, 1877–1888 (2016).
55. Kenerson, H. L., Sullivan, K. M., Labadie, K. P., Pillarisetty, V. G. & Yeung, R. S. Protocol for tissue slice cultures from human solid tumors to study therapeutic response. *STAR. Protocols.* **2**, 100574 (2021).

Acknowledgements

We thank the organ donors and their families for their gift. We thank the staff at the Southwest Transplant Alliance for coordinating DRG recovery from organ donation surgeries, and the members of the Price laboratory tissue recovery team for assistance in DRG recovery.

Author contributions

SP and KG designed and performed experiments and participated in manuscript writing. JM, AM, LM helped with culturing and CRIPSR gRNA design. AC, PH and GF dissected DRGs from organ donors. RK, TJ and AP helped conceptualize, writing and obtaining funding.

Funding

This work was supported by NIH grants U19 NS130608 TJP and R01NS116694 AP.

Declarations

Competing interests

The authors declare no competing interests.

Additional information

Supplementary Information The online version contains supplementary material available at https://doi.org/10.1038/s41598-025-91153-2.

Correspondence and requests for materials should be addressed to T.J.P. or A.P.

Reprints and permissions information is available at www.nature.com/reprints.

Publisher's note Springer Nature remains neutral with regard to jurisdictional claims in published maps and institutional affiliations.

Open Access This article is licensed under a Creative Commons Attribution-NonCommercial-NoDerivatives 4.0 International License, which permits any non-commercial use, sharing, distribution and reproduction in any medium or format, as long as you give appropriate credit to the original author(s) and the source, provide a link to the Creative Commons licence, and indicate if you modified the licensed material. You do not have permission under this licence to share adapted material derived from this article or parts of it. The images or other third party material in this article are included in the article's Creative Commons licence, unless indicated otherwise in a credit line to the material. If material is not included in the article's Creative Commons licence and your intended use is not permitted by statutory regulation or exceeds the permitted use, you will need to obtain permission directly from the copyright holder. To view a copy of this licence, visit http://creativecommons.org/licenses/by-nc-nd/4.0/.

© The Author(s) 2025